JIPB Journal of Integrative Plant Biology

Research Article
https://doi.org/10.1111/jipb.13648

UVR8-TCP4-LOX2 module regulates UV-B tolerance in Arabidopsis

Cheng Li[1,2†], Jiancan Du[1,3†], Huini Xu[4], Zhenhua Feng[1], Caspar C. C. Chater[5], Yuanwen Duan[1*], Yongping Yang[1*] and Xudong Sun[1*]

1. Yunnan Key Laboratory of Crop Wild Relatives Omics, The Germplasm Bank of Wild Species, Kunming Institute of Botany, Chinese Academy of Sciences, Kunming 650201, China
2. University of Chinese Academy of Sciences, Beijing 100049, China
3. CAS Key Laboratory of Tropical Plant Resources and Sustainable Use, Xishuangbanna Tropical Botanical Garden, Chinese Academy of Sciences, Kunming 650223, China
4. Faculty of Life Science and Technology, Kunming University of Science and Technology, Kunming 650031, China
5. Royal Botanic Gardens, Kew, Richmond, Surrey TW9 3AE, UK
†These authors contributed equally to this work.
*Correspondences: Yuanwen Duan (duanyw@mail.kib.ac.cn); Yongping Yang (yangyp@mail.kib.ac.cn); Xudong Sun (sunxudong@mail.kib.ac.cn, Dr. Sun is fully responsible for the distributions of all materials associated with this article)

Cheng Li

Xudong Sun

ABSTRACT

The phytohormone jasmonate (JA) coordinates stress and growth responses to increase plant survival in unfavorable environments. Although JA can enhance plant UV-B stress tolerance, the mechanisms underlying the interaction of UV-B and JA in this response remain unknown. In this study, we demonstrate that the UV RESISTANCE LOCUS 8 - TEOSINTE BRANCHED1, Cycloidea and PCF 4 - LIPOXYGENASE2 (UVR8-TCP4-LOX2) module regulates UV-B tolerance dependent on JA signaling pathway in *Arabidopsis thaliana*. We show that the nucleus-localized UVR8 physically interacts with TCP4 to increase the DNA-binding activity of TCP4 and upregulate the JA biosynthesis gene *LOX2*. Furthermore, UVR8 activates the expression of *LOX2* in a TCP4-dependent manner. Our genetic analysis also provides evidence that TCP4 acts downstream of UVR8 and upstream of *LOX2* to mediate plant responses to UV-B stress. Our results illustrate that the UV-B-dependent interaction of UVR8 and TCP4 serves as an important UVR8-TCP4-LOX2 module, which integrates UV-B radiation and JA signaling and represents a new UVR8 signaling mechanism in plants.

Keywords: anthocyanin accumulation, jasmonic acid, TCP4, UV-B, UVR8

Li, C., Du, J., Xu, H., Feng, Z., Chater, C. C. C., Duan, Y., Yang, Y., and Sun, X. (2024). UVR8-TCP4-LOX2 module regulates UV-B tolerance in *Arabidopsis*. J. Integr. Plant Biol. **00:** 1–12.

INTRODUCTION

Highly energetic shorter wavelengths of solar UV-B cause major damage to global plant productivity, whereas low UV-B irradiation elicits production of secondary metabolism to enhance crop quality (Schreiner et al., 2016; Shamala et al., 2020). The UV-B photoreceptor UV RESISTANCE LOCUS 8 (UVR8) is a plant-specific and highly conserved protein (Rizzini et al., 2011; Jenkins, 2014; Soriano et al., 2018). UV-B absorption by UVR8's tryptophan chromophore causes dissociation of the dimer, enabling monomeric UVR8 to localize to the nucleus and interact with other proteins. In Arabidopsis, UVR8 interacts with constitute photomorphogenesis protein 1 (COP1) in a UV-B-dependent manner, and thereby mediates UV-B signaling (Christie et al., 2012; Huang et al., 2013; Yin et al., 2016). REPRESSOR OF UV-B PHOTOMORPHOGENESIS (RUP) 1 and RUP2 physically interact with UVR8 to mediate UVR8 re-dimerization independently of COP1 and contribute to UV-B tolerance (Heijde and Ulm, 2013; Tissot and Ulm, 2020). Recently, a study has shown that UVR8 physically interacts with MYB73/MYB77 in a UV-B-dependent manner and inhibits lateral root development

via the coordination of UV-B light and auxin signaling (Yang et al., 2020). In the nucleus, UVR8 also physically interacts with WRKY36, BES1 (BRI1-EMS-SUPPRESSOR1), and BIM1 (bes1-INTERACTING MYC-LIKE 1) to regulate photomorphogenesis dependent on brassinosteroid (BR) signaling (Yang et al., 2018; Liang et al., 2020). However, JA may be significantly increased after exposure to UV-B treatment in Arabidopsis (Mackerness et al., 1999). Furthermore, exogenous application of JA can enhance plant UV-B stress tolerance (Demkura et al., 2010; Liu et al., 2012; Quan et al., 2018). The underlying mechanisms interplayed between JA and UV-B/UVR8 signaling are poorly understood.

The TEOSINTE BRANCHED1, Cycloidea and PCF (TCP) family is a plant-specific transcription factor family which regulates leaf morphology, branching, leaf senescence, and petal development. Five CIN-like TCP genes, namely *TCP2*, *TCP3*, *TCP4*, *TCP10* and *TCP24*, are the targets of miR319 (Palatnik et al., 2003). MiR319 and its targets have been found to modulate leaf growth (Palatnik et al., 2003; Ori et al., 2007; Sarvepalli and Nath, 2011; Li et al., 2012; Bresso et al., 2018; Zheng et al., 2022), flower development (Nag et al., 2009; Kubota et al., 2017; Liu et al., 2017), xylem vessel formation (Sun et al., 2017), trichome formation (Vadde et al., 2018; Zhou et al., 2019; Fan et al., 2020; Lan et al., 2021; Saini et al., 2022), and photomorphogenesis (Dong et al., 2019; Saini et al., 2022). *TCP4* is the major target of miR319 (Nag et al., 2009). The miR319-TCP4 module was previously identified as a regulator of cell proliferation, affecting leaf form and size (Schommer et al., 2014). In both *in vivo* and *in vitro* experiments, TCP4 has demonstrated its ability to bind to the promoter of *LIPOXYGENASE2* (*LOX2*) and activate the expression *LOX2*, a gene crucial in the biosynthesis of JA (Schommer et al., 2008; Guo et al., 2018). TCP4 also integrates developmental and environmental signals to promote hypocotyl elongation (Challa et al., 2016). Overexpression of miR319 increased cold tolerance in rice and sugarcane (Thiebaut et al., 2012; Yang et al., 2013), and salt and drought tolerance in creeping bentgrass (*Agrostis stolonifera* L.) and switchgrass (*Panicum virgatum* L.) (Zhou et al., 2013; Liu et al., 2019). Although correlations between the miR319-TCP4 module and stress tolerance have been identified, these remain poorly understood at the molecular level.

In this study, we show that Arabidopsis TCP4 positively regulates UV-B tolerance dependent on JA signaling. We further demonstrate that TCP4 physically interacts with UVR8 in a UV-B-dependent manner, and that the TCP4-UVR8 complex accumulates in nuclei to enhance tolerance to UV-B radiation. Our genetic analysis showed that TCP4 acts downstream of UVR8 and upstream of *LOX2* to regulate JA biosynthesis. Together, these results demonstrate that UV-B light-dependent UVR8-TCP4 interactions enable a coordinated JA signaling response to protect plants against UV-B damage.

RESULTS

TCP4 physically interacts with UVR8

In plants, transcription factors usually function in combination with other protein partners. We first fused TCP4 with the LexA DNA-binding domain (BD) to screen an Arabidopsis complementary DNA (cDNA) library for identification of TCP4-interacting proteins using the yeast two-hybrid (Y2H) system. We found that TCP4 interacted with UVR8 in both darkness and UV-B light (Figure S1). Intriguingly, *jaw*-D mutants, that overexpress miR319, had reduced anthocyanin pigment production, whereas the constitutive expression of miR319-resistant TCP4 (*rTCP4*) resulted in significantly increased production of anthocyanins (Figure S2A, B). We speculated that TCP4 might interact with UVR8 in response to UV-B stress and mediate anthocyanin biosynthesis.

To test this hypothesis, we first examined the tolerance of wild type (WT), *jaw*-D, *rTCP4-3*, and *rTCP4-6* to treatment with UV-B. After UV-B treatment, *rTCP4-3* and *rTCP4-6* were more tolerant to UV-B stress than WT, whereas *jaw*-D was less tolerant to UV-B stress than WT (Figure S2C–E). Second, the interaction between TCP4 and UVR8 was examined using an *in vitro* pull-down assay. The recombinant UVR8^{W285A} (constitutively monomeric UVR8) protein could be pulled down by TCP4 tagged with HIS (TCP4-HIS). Interestingly, the recombinant UVR8 protein could also be pulled down by TCP4-HIS (Figure 1A). The *in vivo* interaction of TCP4 and UVR8 was further confirmed by co-immunoprecipitation (Co-IP). TCP4 was co-immunoprecipitated with UVR8 from leaf tissues irradiated with UV-B light (Figure 1B). A bimolecular luciferase complementation (BiLC) assay confirmed that TCP4 directly interacted with UVR8 in plant cells upon UV-B treatment (Figure 1C, D). We also found that TCP4 interacted with UVR8^{W285A} in the BiLC assay (Figure 1E). These results indicate that TCP4 interacts with UVR8 in the nucleus in a UV-B-dependent manner. As a transcription factor, TCP4 functions in the nucleus, and UV-B is known to promote the nuclear accumulation of UVR8 (Liang et al., 2019). We therefore tested whether UV-B irradiation increases TCP4-UVR8 complex formation in the nucleus. Strong fluorescence was detected in the nuclei of cells co-transformed with TCP4-nGFP and UVR8-cGFP, but no fluorescence was detected in cells co-transformed with TCP4-nGFP and cGFP or nGFP and UVR8-cGFP under UV-B light (Figure 2). These results indicate that UV-B induces the nuclear accumulation of UVR8 and promotes TCP4-UVR8 complex formation in the nucleus.

TCP4 establishes UV-B tolerance alongside UVR8

To determine the biological roles of TCP4 under UV-B, we first examined whether UV-B affected *TCP4* expression. Expression levels of *TCP4* increased about twofold within the first hour of UV-B light irradiation and then decreased, and this followed a similar expression pattern to *UVR8* (Figure 3A). To confirm the effect of UVR8 on *TCP4* expression, we first examined the expression level of *TCP4* in the *uvr8* mutant. The results showed no significant difference in *TCP4* expression levels

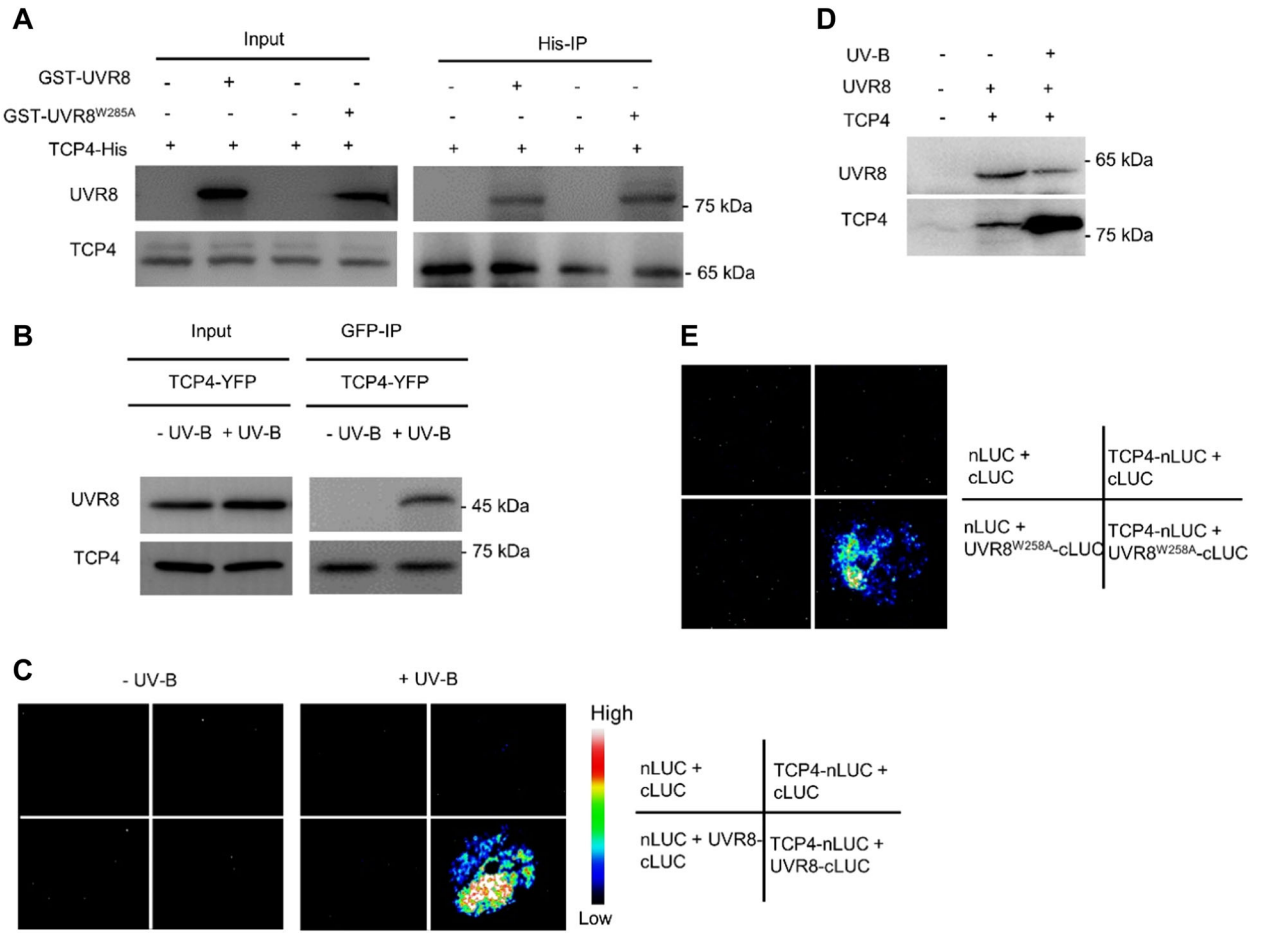

Figure 1. TEOSINTE BRANCHED1, Cycloidea and PCF 4 (TCP4) physically interacts with UV RESISTANCE LOCUS 8 (UVR8)
(A) TCP4 interacts with UVR8 by pull-down assays. TCP4-His bound to His beads was mixed with glutathione S-transferase (GST)-UVR8 purified from *Escherichia coli*. **(B)** Co-immunoprecipitation (Co-IP) assays using 14-d-old transgenic seedlings expressing *pER8-TCP4-EYFP* treated with or without UV-B for 30 min. Input: immunoblots showing the level of TCP4-YFP (yellow fluorescent protein) and UVR8 in the total protein extract. Green fluorescent protein (GFP)-IP, the IP products precipitated by the GFP antibody. Input or IP products were probed with an anti-GFP or anti-UVR8 antibody. **(C)** Bimolecular luciferase complementation (BiLC) assays showing the interaction between TCP4 and UVR8 in *Nicotiana benthamiana* under UV-B light. **(D)** Western blot of whole cell extracts from co-injection of TCP4 and UVR8 in **(C)**. **(E)** BiLC assay showing that TCP4 interacts with UVR8^{W285A} in white light (without UV-B). −UV-B, without UV-B; +UV-B, treatment with UV-B.

under UV-B treatment (Figure 3B). Thus, the transient transcription assays were conducted in tobacco leaves. *ProTCP4:LUC* alone or in combination with *35S:UVR8* did not show any obviously different luciferase (LUC) activity without UV-B radiation. However, co-introduction of *35S:UVR8* with *ProTCP4:LUC* led to increasing LUC activity in response to UV-B radiation (Figure 3C). These results indicate that UV-B light induces the transcription of *TCP4* in a UVR8-dependent manner. We next investigated genetic interactions between *TCP4* and *UVR8* genes. The *uvr8* mutant was crossed with *rTCP4-3*, resulting in *rTCP4-3/uvr8* (Figure S3). In the absence of UV-B, the phenotype of the *rTCP4-3/uvr8* genotype was not affected (Figure 3D, E, G). Most strikingly, we observed that *rTCP4-3* plants were more tolerant to UV-B stress than WT, and overexpression of *rTCP4* in *uvr8* mutants partially restored *uvr8* tolerance to UV-B irradiation (Figure 3F, G). These results indicated that TCP4 contributes to UV-B tolerance, which is partially dependent on UVR8.

TCP4 plays a positive role in UV-B tolerance dependent on *LOX2*

Previous studies demonstrated that TCP4 can directly bind to the promoter of *LIPOXYGENASE2* (*LOX2*) (Schommer et al., 2008; Guo et al., 2018). As *LOX2* is a JA biosynthetic gene, and JA mediates anthocyanin accumulation via regulating the WD40/bHLH/R2R3-MYB (WBM) complex (Qi et al., 2011), this suggests that TCP4 might mediate anthocyanin biosynthesis via JA signaling. We therefore analyzed JA content and *LOX2* expression in genotypes with contrasting *TCP* expression. JA content and *LOX2* expression in *jaw*-D mutants was lower than that of wild type (WT) plants, whereas *rTCP4* overexpression lines possessed higher JA concentrations and *LOX2* expression than WT plants (Figure S4), which were in agreement with their relative anthocyanin contents.

To study genetic interactions in JA-mediated anthocyanin biosynthesis, *rTCP4-3* was crossed with the low-anthocyanin *lox2* mutant to generate *rTCP4-3/lox2* plants. Overexpression

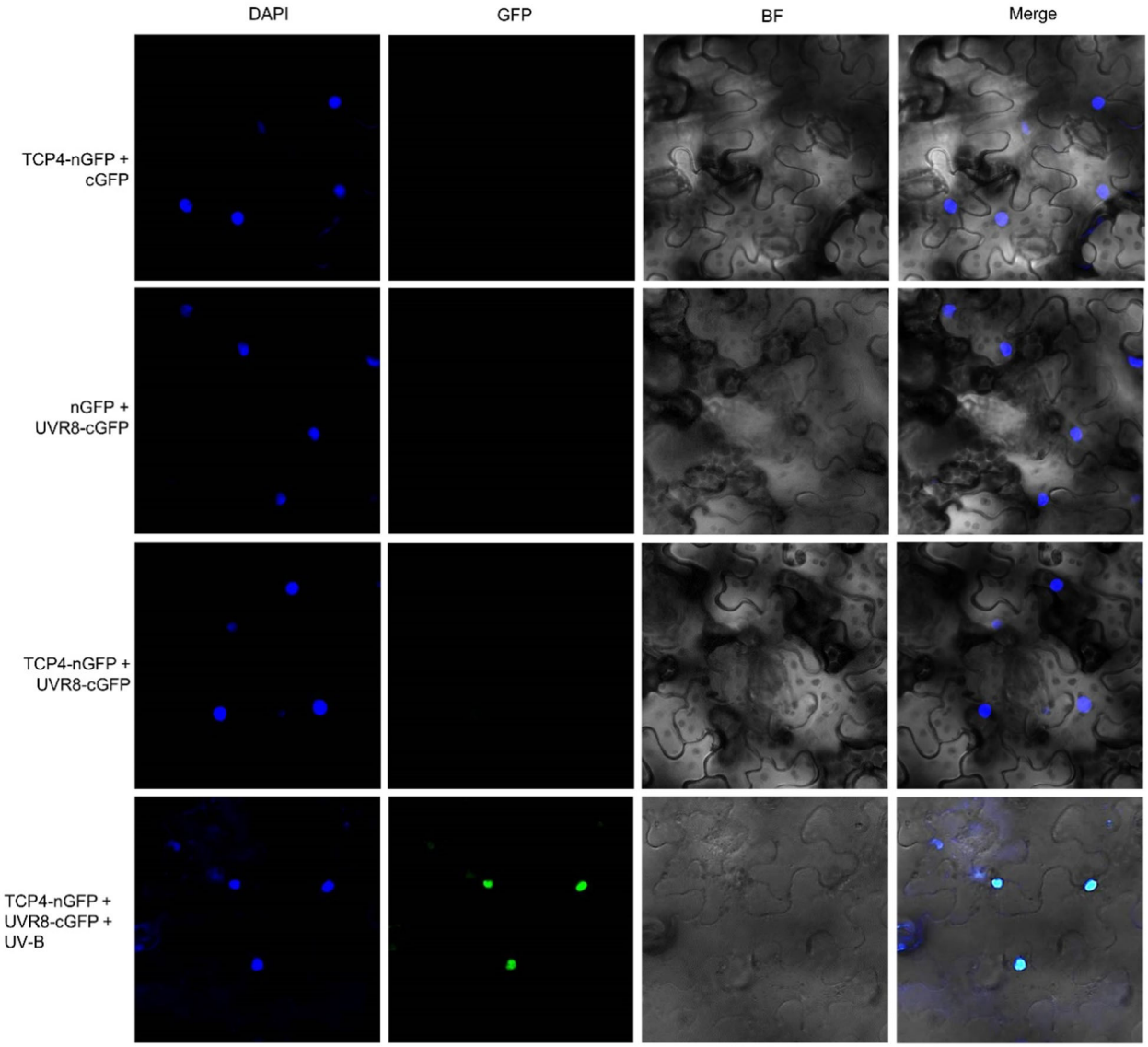

Figure 2. UV-B promotes the formation of the TEOSINTE BRANCHED1, Cycloidea and PCF 4 - UV RESISTANCE LOCUS 8 (TCP4-UVR8) complex in nucleus

Bimolecular fluorescence complementation (BiFC) assays showing that UV-B treatment promotes the formation of a TCP4-UVR8 complex. The leaves of *Nicotiana benthamiana* were co-transformed with TCP4-nGFP and UVR8-cGFP and treated with (2 W/m^2) or without UV-B for 10 min before imaging. DAPI, 4′,6-diamidino-2-phenylindole staining. BF, bright field; GFP, green fluorescence protein; Merge, overlay of the DAPI, GFP, and BF images.

of *rTCP4-3* in the *lox2* background failed to restore anthocyanin biosynthesis of *lox2* (Figures 4A, S5). In contrast, treatment with methyl JA (MeJA) rescued anthocyanin accumulation in both the *lox2* and *rTCP4-3*/*lox2* genotypes (Figures 4B, S5). Quantitative real-time polymerase chain reaction (qRT-PCR) analysis showed that TCP4 cannot activate the expression of WBM genes in the absence of *LOX2* (Figure S6). These results indicate that TCP4 activates the expression of WBM genes dependent on the LOX2-mediated JA signaling pathway.

Given that UV-B exposure contributes to anthocyanin biosynthesis, we investigated whether higher anthocyanin content increases UV-B resistance. In the absence of UV-B, the phenotype and survival rates of WT, *lox2* *rTCP4-3*, and *rTCP4-3*/*lox2* plants were not obviously different (Figure 4C, D, G). However, when these genotypes were grown under UV-B radiation, the survival rate of *rTCP4-3* seedlings was approximately 400% greater than WT seedlings, and almost all *lox2* mutants died. Overexpression of *rTCP4* in *lox2* plants failed to enhance UV-B resistance (Figure 4E, F, G). These results indicate that TCP4 enhances the tolerance of UV-B radiation dependent on JA signaling.

UVR8 activates *LOX2* expression dependent on TCP4

The interaction between TCP4 and UVR8 prompted us to determine whether UVR8 affected the transcriptional activity

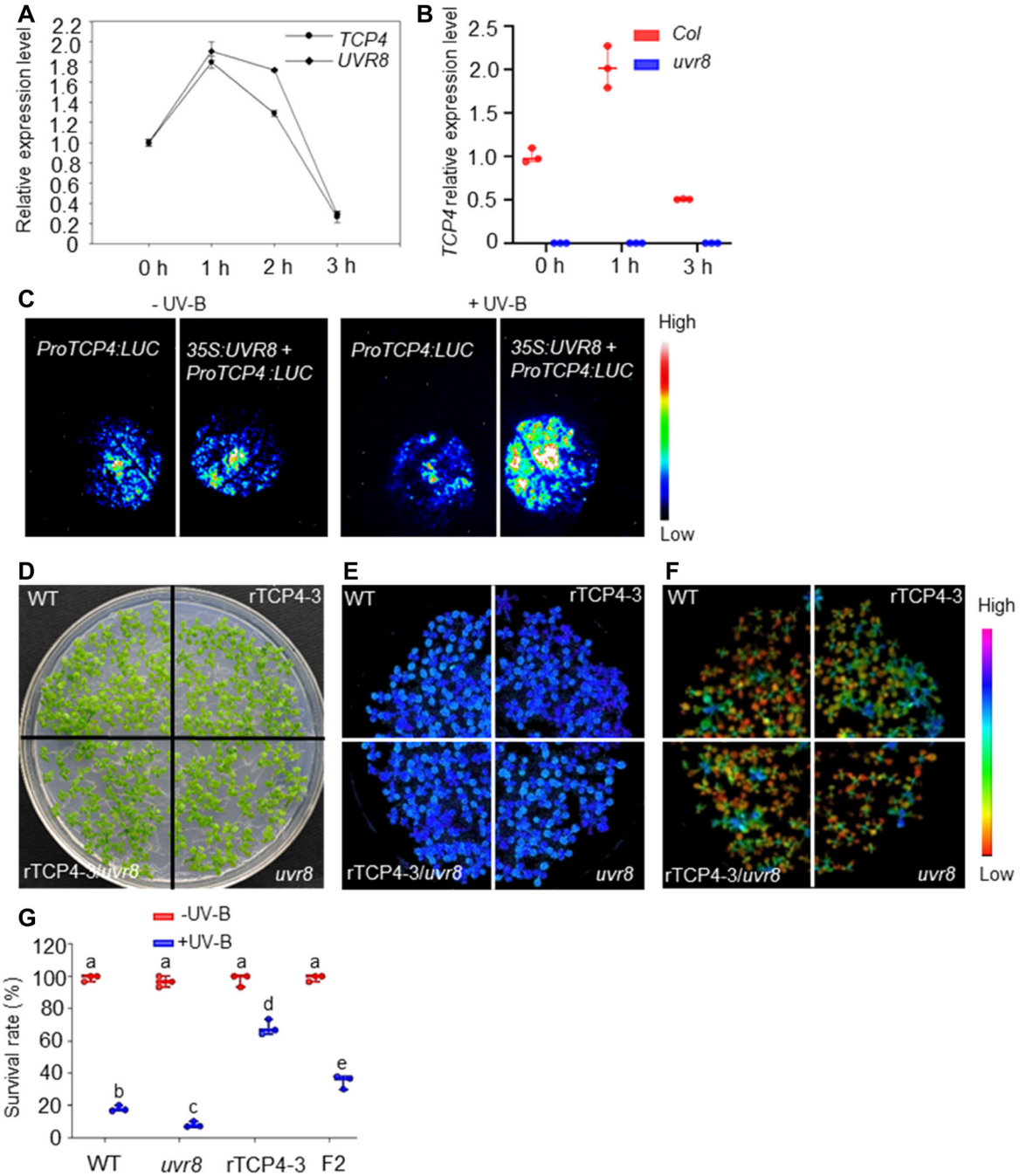

Figure 3. TEOSINTE BRANCHED1, Cycloidea and PCF 4 (TCP4) acts downstream of UV RESISTANCE LOCUS 8 (UVR8) in response to UV-B stress

(A) Quantitative real-time polymerase chain reaction (qRT-PCR) results showing that transcripts of *TCP4* and *UVR8* have similar expression patterns under UV-B (2 W/m^2) radiation. Seven-d-old seedlings were grown in white light, then treated with UV-B for the indicated time. Error bars indicate ± *SE* ($n = 3$). **(B)** qRT-PCR results showing that transcript of *TCP4* is dependent on UVR8 under UV-B radiation. Seven-d-old seedlings were grown in white light, then treated with UV-B for the indicated time. Error bars indicate ± *SE* ($n = 3$). **(C)** UV-B induced transcription of *TCP4* in a UVR8-dependent manner. Leaf epidermal cells of *Nicotiana benthamiana* were transfected with *ProTCP4:LUC* or *ProTCP4:LUC* together with *35S:UVR8* and treated with or without UV-B (2 W/m^2) for 10 min before imaging. **(D)** Phenotype of seedlings of the indicated genotypes were grown in the presence of white light for 7 d. **(E)** Chlorophyll fluorescence (Fv/Fm) of seedlings of the indicated genotypes in **(D)** were captured before UV-B treatment. **(F)**, Fv/Fm of the indicated genotypes were captured in **(D)** after 3 d treatment with UV-B (3 W/m^2) for 6 h. rTCP4-3/*uvr8* (*rTCP4*-overexpressing plants in the genetic background of *uvr8*). The false color code depicted at the right of the image ranges from 0 (black) to 1 (purple) as a viability/mortality indicator. **(G)** Survival rate of indicated genotypes in **(E, F)**. Data presented are the means ± *SD* ($n = 30$) of three independent experiments. Shared letters indicate no statistically significant difference in the means ($P > 0.05$).

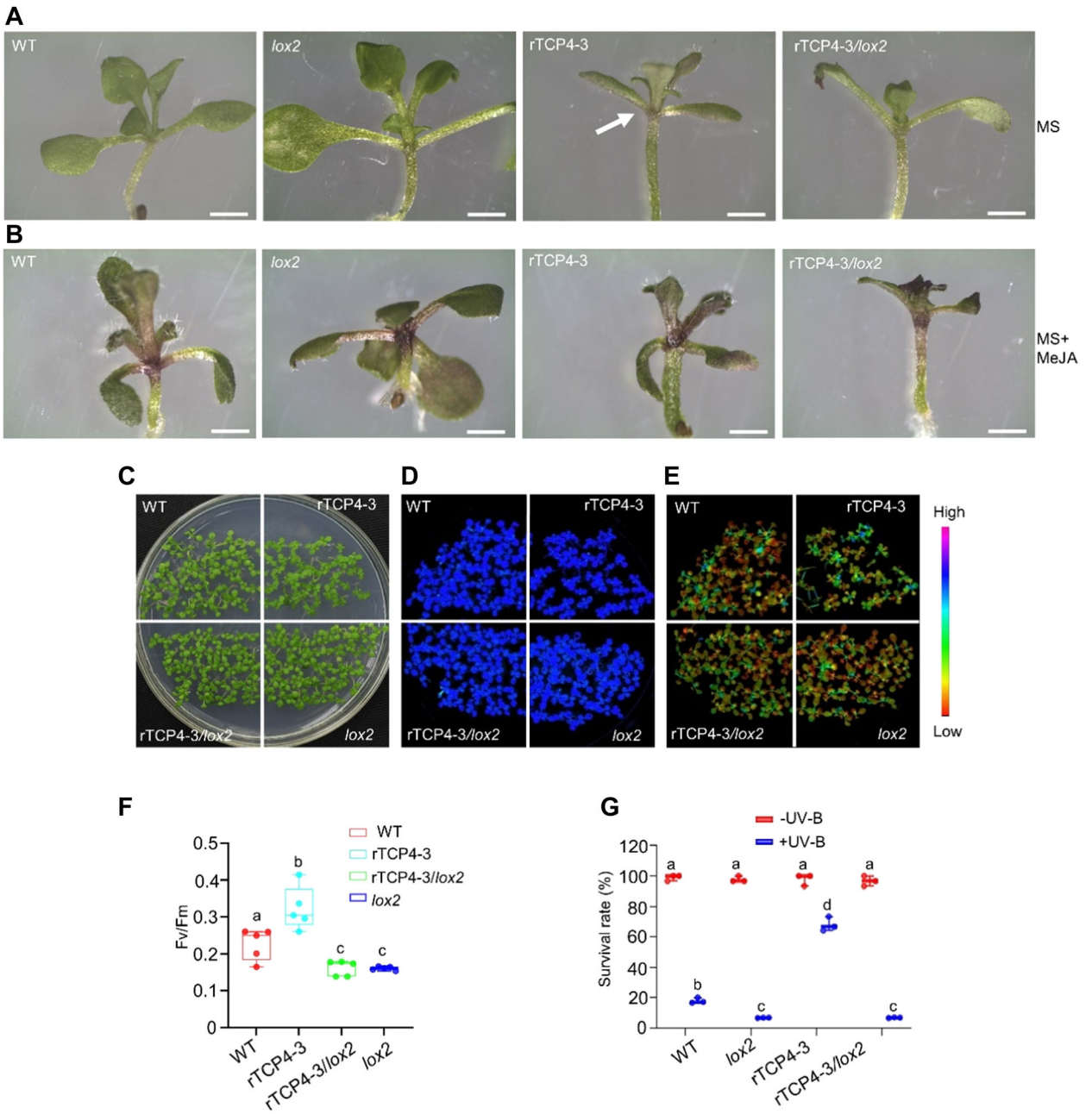

Figure 4. TEOSINTE BRANCHED1, Cycloidea and PCF 4 (TCP4) acts upstream of *LOX2* in response to UV-B stress

(A) Ten-d-old seedlings grown on Murashige and Skoog (MS) supplied without methyl jasmonate (MeJA). **(B)** Ten-d-old seedlings grown on MS supplied with 25 μmol/L MeJA. Bars = 0.2 cm. **(C)** Phenotype of seedlings of the indicated genotypes were grown in white light for 7 d. **(D)** Chlorophyll fluorescence (Fv/Fm) of seedlings of the indicated genotypes in **(C)** were captured before UV-B treatment. **(E)** Fv/Fm of the indicated genotypes were captured in **(C)** after 3 d treatment with UV-B (3 W/m^2) for 6 h. rTCP4-3/*lox2* (*rTCP4*-overexpressing plants in the genetic background of *lox2*). The false color code depicted at the bottom of the image ranges from 0 (black) to 1 (purple) as a viability/mortality indicator. **(F)** Photosynthetic traits of Fv/Fm in **(E)**. **(G)** Survival rate of indicated genotypes in **(E)**. Data presented are the means ± *SD* ($n = 30$) of three independent experiments. Shared letters indicate no statistically significant difference in the means ($P > 0.05$).

of *TCP4*. We first examined the expression level of *LOX2* in WT and *jaw*-D under UV-B irradiation. When continuous white light-grown seedlings were exposed to UV-B light, the expression level of *LOX2* in WT seedlings increased within the first hour of UV-B light irradiation (Figure 5A), which is reminiscent of the WT *TCP4* expression pattern in response to UV-B (Figure 3A). However, the expression level of *LOX2* in *jaw*-D seedlings (with constitutively lower *TCP4* levels) was lower than that in the WT, and did not show obvious differences among different treatment times (Figure 5A). We also performed transient expression in *Nicotiana benthamiana* to analyze the involvement of UVR8 in the association of TCP4 with the *LOX2* promoter. We found that UVR8 could not activate the expression of *LOX2* by itself, but UVR8 could enhance the expression level of *LOX2* when UVR8

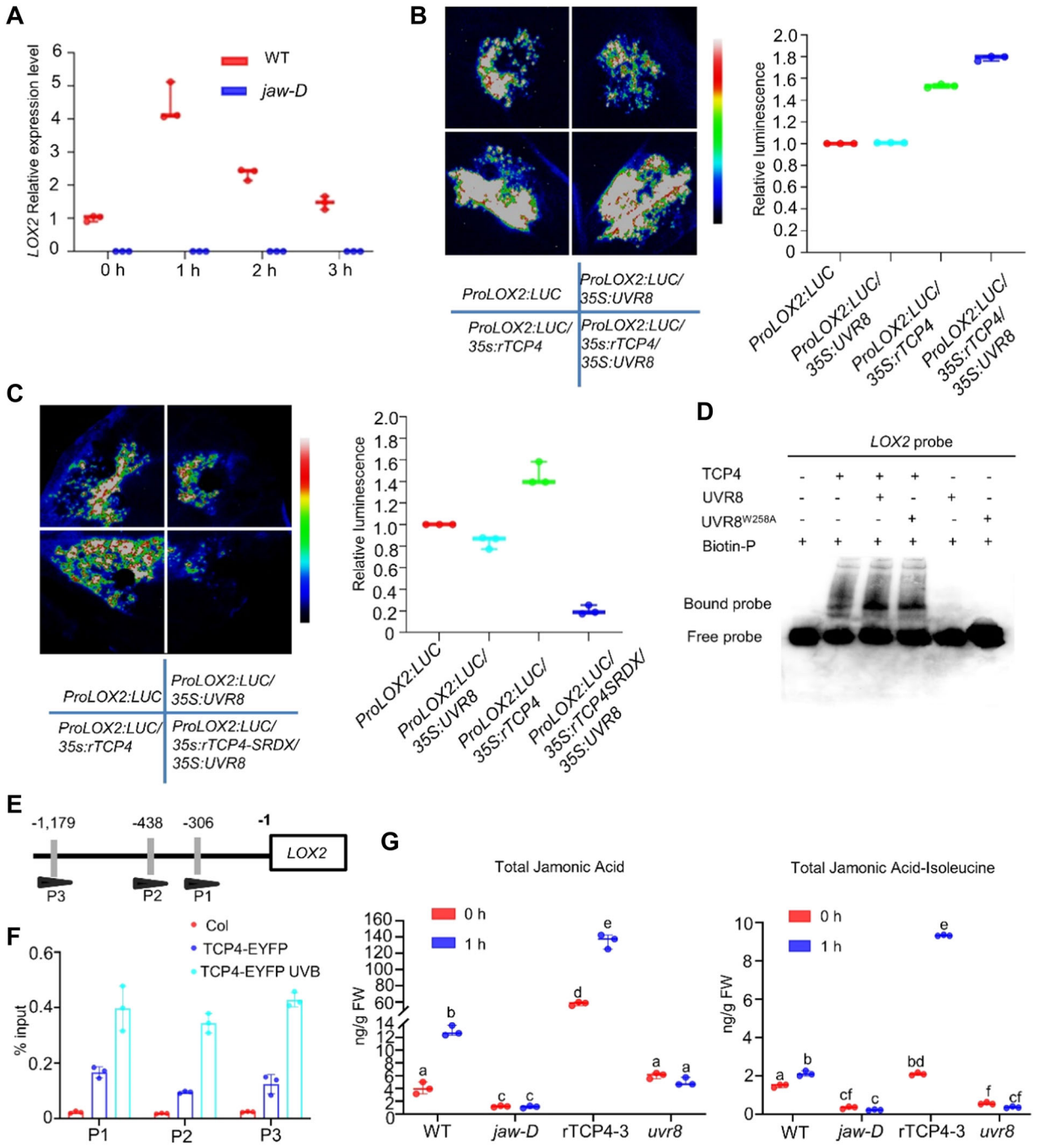

Figure 5. UV RESISTANCE LOCUS 8 (UVR8) activates *LOX2* expression dependent on TEOSINTE BRANCHED1, Cycloidea and PCF 4 (TCP4)

(A) Quantitative real-time polymerase chain reaction (qRT-PCR) results showing that the expression of *LOX2* is regulated by TCP4 under UV-B radiation. Seven-d-old seedlings were grown in white light, then treated with UV-B for the indicated time. Error bars indicate ± *SE* ($n = 3$). **(B)** Transient expression of the *35S:TCP4* and/or *35S:UVR8* effector constructs with the *ProLOX2:LUC* reporter construct in *Nicotiana benthamiana* leaves. UVR8 increases the transcriptional activity of TCP4 under UV-B treatment. **(C)** Transient expression of the *35S:TCP4-SRDX* and/or 35S:UVR8 effector constructs with the *ProLOX2:LUC* reporter construct in *N. benthamiana* leaves. UVR8 activates the *LOX2* expression dependent on TCP4. **(D)** Electrophoresis mobility shift assay showing that both UVR8 and UVR8^{W258A} could enhance the DNA-binding activity of TCP4. Biotin-P indicates the biotin-labeled probe. **(E)** Schematic of the location of TCP4-binding motif in the promoter of *LOX2* gene. Solid arrowheads indicate TCP4-binding sites. P1, P2, and P3 represent the fragments amplified in **(F)**. **(F)** Chromatin immunoprecipitation assay of TPC4 binding to the promoter region of *LOX2* in 2-week-old pER8-TCP4-EYFP and wild type leaves in white light or moved to white light plus UV-B (1 W/m^2) for 30 min. Relative enrichment was calculated as the value of the amplified signal normalized against that of the input DNA. Data presented are the means ± *SD* of three biological replicates. **(G)** Jasmonate (JA) concentrations were measured using high-performance liquid chromatography – tandem mass spectrometry in 2-week-old wild type (WT), *jaw*-D, rTCP4-3, and *uvr8* plants in white light or moved to white light plus UV-B (1 W/m^2) for 1 h. Data presented are the means ± *SD* of three biological replicates.

and TCP4 co-transformed (Figure 5B). The luminescence intensity was inhibited when UVR8 and TCP4-SRDX (SRDX, transcriptional repressor domain) co-transformed (Figure 5C). Next, we performed an electrophoresis mobility shift assay (EMSA) using recombinant TCP4, UVR8, and UVR8^{W285A} in *Escherichia coli*. TCP4 bound to the TCP binding site of the *LOX2* promoter. Interestingly, not only UVR8^{W285A} but also UVR8 could enhance the binding of TCP4 to the *LOX2* promoter (Figure 5D). A chromatin immunoprecipitation (ChIP) assay was conducted to evaluate the potential binding of TCP4 to P1, P2, and P3 motifs (Figure 5E) *in vivo*. The ChIP-quantitavive polymerase chain reaction analysis revealed that the DNA fragments containing P1, P2, and P3 motifs were enriched in plants expressing TCP4-YFP (yellow fluorescent protein), with significantly higher enrichments observed after UV-B treatment (Figure 5F). These results indicate that UV-B may facilitate the binding of TCP4 to the *LOX2* promoter. Subsequently, the content of JA was measured in WT, *jaw*-D, rTCP4-3, and *uvr8* plants following UV-B treatment. The JA concentrations in *jaw*-D, and *uvr8* mutants did not show significant differences after UV-B treatment, while the JA levels in rTCP4-3 significantly increased upon UV-B treatment (Figure 5G). These observations imply that both UV-B and UVR8 influence JA levels through TCP4. This is consistent with the notion that UVR8 triggers the expression of *LOX2* in a TCP4-dependent manner.

DISCUSSION

TCP4, which belongs to the CIN subfamily, is the major target of miR319. TCP4 has been well elucidated to regulate cell proliferation, hypocotyl elongation, secondary cell wall formation, and flowering time (Schommer et al., 2014; Challa et al., 2016; Kubota et al., 2017; Liu et al., 2017; Sun et al., 2017). Previous observations have shown TCP4 to bind to the promoter of *LOX2 in vivo* and *in vitro* (Schommer et al., 2008; Guo et al., 2018). LOX2 is involved in the initial step in JA biosynthesis, which catalyses the oxidation of α-linoleic acid to 13 (S)-hydroperoxylinolenic acid. *LOX2* has been shown to be strongly induced by wounding (Schommer et al., 2008; Glauser et al., 2009), but the mutation of TCP4-binding sites in the *LOX2* promoter does not attenuate wounding-induced *LOX2* expression, which indicates that TCP4 is not involved in the wound response (Schommer et al., 2008). Senescence, determined by chlorophyll loss and *SAG12* expression, did not differ between WT and LOX2-RNAi (RNA interference) plants (Seltmann et al., 2010). These results suggest that TCP4-LOX2 is not involved in wounding responses or senescence. Until now, the deleterious phenotypes of *rTCP4:GFP* transgenic plants have precluded the collection of sufficient material for JA measurements (Schommer et al., 2008). Hence, the physiological function of the miR319-targeted TCP4 transcription factor in Arabidopsis JA biosynthesis remains unknown.

Jasmonate is an important phytohormone involved in plant development and environmental adaptation (Hu et al., 2017). JA induces the degradation of JAZ proteins dependent on the SCF^{COI1}-26S proteasome pathway, after which WBM complexes are released from the JAZ-WBM complex to activate the expression of anthocyanin biosynthesis genes (Qi et al., 2011). Previous studies have shown that TCP4 can directly bind to the *LOX2* promoter (Schommer et al., 2008; Guo et al., 2018). Overexpression of *rTCP4* in WT plants induces early-onset senescence before maturity (Schommer et al., 2008), suggesting that TCP4-targeted *LOX2* may play a role in senescence. However, Seltmann et al. (2010) have demonstrated that *LOX2* is not required for senescence to occur. In the present study, we found that overexpression of *rTCP4* increases JA content and anthocyanin accumulation, which suggests that TCP4 might mediate anthocyanin accumulation through a LOX2-mediated JA signaling pathway. As JA regulates anthocyanin accumulation via WBM complexes, we performed transcriptional analysis to show that *rTCP4* overexpression upregulated WBM complex genes encoding basic helix-loop-helix (bHLH) transcription factors (TT8, GL3 and EGL3) and R2R3 MYB transcription factors (MYB75 and GL1). The expression levels of these WBM complex genes were disrupted in *lox2* plants, and *rTCP4* overexpression in *lox2* failed to rescue their transcription. Genetic analysis showed that overexpression of *rTCP4* in *lox2* could not recover anthocyanin accumulation in *lox2*. After MeJA treatment, *lox2* and *rTCP4-3/lox2* plants could accumulate anthocyanin normally, strongly suggesting that TCP4 regulates anthocyanin accumulation through the LOX2-mediated JA signaling pathway.

UVR8 does not possess a DNA-BD, and the interaction between UVR8 and transcription factors (TFs) enables UVR8 to be involved in transcriptional regulation. The UVR8-COP1 interaction stabilizes HY5 to elicit UV-B-responsive gene expression (Ren et al., 2019). Similarly, UVR8-WRKY36 interaction alleviates WRKY36 repression of *HY5* expression, and inhibits hypocotyl elongation (Yang et al., 2018), whereas the UVR8-BES1/BIM1 interaction inhibits BR-responsive gene expression for cell elongation to promote UV-B-induced photomorphogenesis (Liang et al., 2018, 2020). Recently, two studies reported that UVR8 interacts with different MYB TFs in roots and cotyledons to regulate lateral root growth and cotyledon development, respectively (Qian et al., 2020; Yang et al., 2020). In each case, the interaction is enhanced by UV-B light and alters the DNA-binding activity of the transcription factor. We also found that UVR8 could enhance the DNA-binding activity of TCP4 under UV-B irradiation. *jaw*-D plants, in which *TCP4* is downregulated, are hypersensitive to UV-B stress, while *TCP4*-overexpressing plants are more tolerant to UV-B. However, hypocotyls of *rTCP4*-overexpressing plants are longer than those of WT plants, indicating that TCP4 regulates UV-B tolerance independently of HY5 signaling. However, overexpression of *rTCP4* in *uvr8* mutants could not completely restore *uvr8* tolerance to UV-B irradiation. Therefore, we speculate that TCP4-*LOX2* pathway acts redundantly with HY5 pathway under UV-B radiation. Our Co-IP and BiLC results showed that the interaction between TCP4 and UVR8 is UV-B-dependent. TCP4, a transcription factor, is localized to the nucleus, and UV-B-light-triggered nuclear

localization of UVR8 allows the interaction between TCP4 and UVR8 *in vivo*. Our results establish a new UV-B signaling pathway, through which UVR8 enhances the binding of TCP4 to the *LOX2* promoter *in vivo* to promote *LOX2* transcription and increase anthocyanin biosynthesis to enhance UV-B tolerance.

Based on our phenotypic and molecular analyses, we propose a working model for the UVR8-TCP4-LOX2 module in the regulation of UV-B-induced anthocyanin biosynthesis and stress response (Figure 6). UV-B light induces the nuclear localization of UVR8, and nuclear-localized UVR8 interacts with TCP4 to promote DNA-binding to the *LOX2* promoter to induce *LOX2* expression. Thereafter, JA biosynthesis releases the MBW complexes to activate their respective downstream genes, leading to anthocyanin biosynthesis. At the same time, TCP4 represses cell proliferation, enabling the plant to allocate energy from growth to anthocyanin biosynthesis and activate defense responses.

MATERIALS AND METHODS

Plant materials and growth conditions

The *Arabidopsis thaliana jaw-D*, *rTCP4-3*, *rTCP4-6* transgenic plants were previously described (Sun et al., 2017). The *lox2* mutant (CS3748) was obtained from the Arabidopsis Biological Resource Center (ABRC). The *rTCP4-3*/*lox2* lines were obtained by crossing *rTCP4-3* transgenic plants with *lox2* plants. *uvr8-6* (SALK_033468) and UVR8^{W285A} (constitutively monomeric UVR8) were kindly provided by Hongtao Liu (Yang et al., 2020). *pER8-TCP4-EYFP* transgenic plants were kindly provided by Aiwu Dong (Li et al., 2012). *ProLOX2:LUC* plasmids were kindly provided by Chuanyou Li (Zhai et al., 2013). All seeds underwent imbibition and subsequently cold-treated at 4°C for a duration of 2 d in the dark prior to germination under light conditions. All plants were cultivated on soil or Murashige and Skoog (MS) agar medium, which was supplemented with 1% sucrose. The cultivation was carried out under a 16-h light and 8-h dark photoperiod at 23°C.

Seven-d-old seedlings of the indicated genotypes were exposed to UV-B radiation at an intensity of 3 W/m^2 for 6 h and allowed to recover for 3 d. Chlorophyll fluorescence (Fv/Fm) of the indicated genotypes was captured used IMAGING-PAM (WALZ, Effeltrich, Germany) before and after treatment with UV-B. The photosynthetic capability was assessed by measuring Fv/Fm. All experiments were conducted with a minimum of three biological replicates.

Quantitative real-time polymerase chain reaction analysis

Total RNA was isolated from 3-week old plant tissues using Eastep® Super Total RNA extract kit (Promega, Beijing, China). First-strand cDNA was synthesized utilizing the GoScript™ Reverse Transcription System (Promega). Transcript quantification was conducted through qRT-PCR analysis with 1/20th of the cDNA as template. The housekeeping gene *ACT2* served as internal standard. Independent plant samples were subjected to triplicate replicates. All primers employed in this study are listed in Table S1.

Transient expression in *N. benthamiana*

Transient expression assays conducted on *N. benthamiana* leaves were executed following the protocol outlined by Sun et al. (2017), with the experiment repeated three times, yielding consistent results.

Anthocyanin measurement

Anthocyanin content of different lines was measured according to Teng et al. (2005). Absorbances at 530 and 650 nm were measured using a spectrophotometer. Anthocyanin quantity = $(A_{535} - A_{650})$ per gram fresh weight.

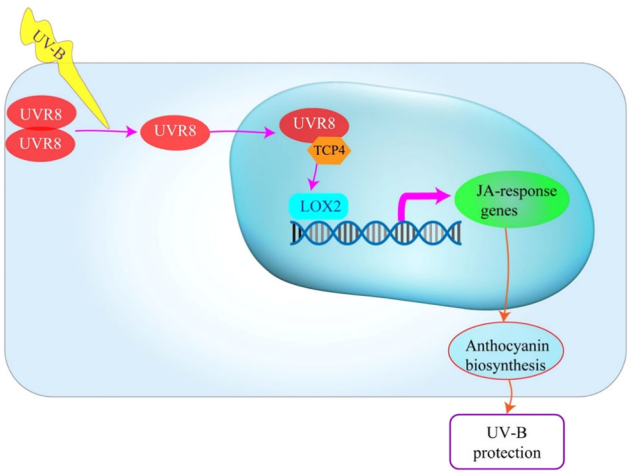

Figure 6. A proposed working model depicting how TEOSINTE BRANCHED1, Cycloidea and PCF 4 (TCP4) acts with UV RESISTANCE LOCUS 8 (UVR8) to mediate UV-B response in Arabidopsis

In response to UV-B light, monomerized UVR8 accumulates in the nucleus and interacts with TCP4, which then enhances TCP4 affinity with the *LOX2* promoter to increase jasmonic acid levels and promotes anthocyanin biosynthesis to improve plant resistance against UV-B stress.

Analysis of JA and JA-Ile/JA-Leu accumulation

Five rosette leaves from the specified plants were used as a biological repeat. Approximately 300 mg of each sample was harvested and flash-frozen in liquid nitrogen. JA and JA-Ile/JA-Leu were subsequently isolated using ethyl acetate, spiked with labeled internal standards ($^{13}C_2$-JA and $^{13}C_6$-JA-Ile, each with 100 ng), in accordance with the method delineated by Qi et al. (2016) and then analyzed by high-performance liquid chromatography – tandem mass spectrometry.

Yeast two-hybrid assay

The appropriate vector combinations were co-transformed into the yeast strain AH109 (Clontech, Beijing, China), and interactions were assessed by growth on fully selective media for a duration of 3 d at 30°C with or without 0.1 μmol/m^2/s narrowband UV-B.

In vitro pull-down

The complete coding sequences of *TCP4*, *UVR8*, and *UVR8*^{W285A} were successfully cloned into pET28a and pGEX-6P1, respectively. These proteins were subsequently expressed and purified from *E. coli* BL21. The protein complex formed between TCP4-His and glutathione S-transferase (GST)-UVR8 was incubated under either white light or white light plus UV-B for 30 min. To isolate the protein complexes, anti-His antibodies were employed, followed by washing to remove unbound protein. The bound proteins were then eluted and subjected to analysis using an immunoblot, which was probed with an anti-UVR8 antibody. Before conducting sodium dodecyl sulfate polyacrylamide gel electrophoresis, samples were subjected to boiling.

Electrophoresis mobility shift assay

A DNA probe was synthesized through the end-labeling of a double-stranded oligo (5′-tcagatcctGGACCACtgcaataa-3′), which contains a TCP4-binding site and is tagged with a biotin label at the 3′ end. The binding reaction was carried out in a 20 μL total volume comprising 50 fmol of the probe, 1x binding buffer (comprising 20 mmol/L HEPES-KOH, pH 7.8, 100 mmol/L KCl, 1 mmol/L ethylenediaminetetraacetic acid (EDTA), 0.1% bovine serum albumin (BSA), 10 ng herring sperm DNA, and 10% glycerol), and 2 μg of purified protein. After a 30-min incubation at room temperature, the mixture was loaded onto a 6% native polyacrylamide gel. Electrophoresis was carried out at 6 V/cm for 45 min with 0.25x Tris-borate buffer at room temperature.

Co-immunoprecipitation

The Co-IP procedure were executed following the protocol outlined by Yang et al. (2020). For Co-IP, 14-d-old WT and *pER8-TCP4-EYFP* seedlings, cultivated under long day conditions, were exposed to white light alone or white light combined with UV-B (1 W/m^2) for 30 min. Subsequently, the seedlings were ground in liquid nitrogen, homogenized in binding buffer (comprising 25 mmol/L Tris-HCl, 150 mmol/L NaCl, 1 mmol/L EDTA, 1 mM dithiothreitol (DTT), 0.5% (v/v) NP-40, and 1 mmol/L phenylmethylsulfonyl fluoride (PMSF)), and incubated with 30 μL GFP-Trap (ChromoTek, Germany) at a temperature of 4°C for 60 min. The magnetic beads were rinsed three times using protein extraction buffer, and the eluted precipitates were collected in 100 μL of loading buffer for immunoblot analysis.

Bimolecular fluorescence complementation assay and BiLC assay

TCP4 or UVR8 was fused to the C or N terminus of GFP or LUC, respectively, and subsequently transformed into Agrobacterium strain GV3101. *N. benthamiana* plants were cultivated for a period of 3 d post-infiltration. Confocal laser scanning microscopy was conducted utilizing epi-fluorescence microscopy (Olympus 80i, Olympus Corporation, Tokyo, Japan). The leaves were infiltrated with luciferin solution and imaged using a Tanon 5200 S Luminescent Imaging Workstation. Each interaction pair was analyzed with three biological replicates, and one representative result was presented.

Chromatin immunoprecipitation-quantitavive polymerase chain reaction

Chromatin immunoprecipitation was carried out following the method described by Guo et al. (2020). For ChIP assay, 14-d-old WT and pER8-TCP4-EYFP seedlings, cultivated under long day conditions, were exposed to white light or white light combined with UV-B (1 W/m^2) for 30 min. Anti-GFP antibody (ab290, Abcam, Shanghai, China) was used for immunoprecipitation. The polymerase chain reaction primers specific to the TCP4 target gene are listed in Table S1.

ACKNOWLEDGEMENTS

We would like to express our gratitude to Prof. Hongtao Liu, Aiwu Dong, and Chuanyou Li for their support in providing the materials used in this study. We thank ABRC for Arabidopsis mutants. This work was supported by the Second Tibetan Plateau Scientific Expedition and Research (STEP) program (2019QZKK0502), the National Natural Science Foundation of China (No. 32370405).

CONFLICTS OF INTEREST

The authors declare no conflicts of interest.

AUTHOR CONTRIBUTIONS

X.S. and Y.Y. designed the research. C.L., J.D., H.X., Z.F., and Y.Y. performed the experiments. X.S., Y.-W.D., C.L., J. D., and H.X. analyzed the data. X.S., Y.-W.D. and C.C.C.C. wrote the manuscript with comments from all authors. All authors read and approved the contents of this paper.

Edited by: Hongtao Liu, Center for Excellence in Molecular Plant Sciences, Institute of Plant Physiology and Ecology, CAS, China.

Received Nov. 16, 2023; **Accepted** Mar. 1, 2024

REFERENCES

Bresso, E.G., Chorostecki, U., Rodriguez, R.E., Palatnik, J.F., and Schommer, C. (2018). Spatial control of gene expression by miR319-regulated TCP transcription factors in leaf development. Plant Physiol. **176:** 1694–1708.

Challa, K.R., Aggarwal, P., and Nath, U. (2016). Activation of YUCCA5 by the transcription factor TCP4 integrates developmental and environmental signals to promote hypocotyl elongation in Arabidopsis. Plant Cell **28:** 2117–2130.

Christie, J.M., Arvai, A.S., Baxter, K.J., Heilmann, M., Pratt, A.J., O'Hara, A., Kelly, S.M., Hothorn, M., Smith, B.O., Hitomi, K., et al. (2012). Plant UVR8 photoreceptor senses UV-B by tryptophan-mediated disruption of cross-dimer salt bridges. Science **335:** 1492–1496.

Demkura, P.V., Abdala, G., Baldwin, I.T., and Ballaré, C.L. (2010). Jasmonate-dependent and -independent pathways mediate specific effects of solar ultraviolet B radiation on leaf phenolics and antiherbivore defense. Plant Physiol. **152:** 1084–1095.

Dong, J., Sun, N., Yang, J., Deng, Z., Lan, J., Qin, G., He, H., Deng, X. W., Irish, V.F., Chen, H., et al. (2019). The transcription factors TCP4 and PIF3 antagonistically regulate organ-specific light induction of SAUR genes to modulate cotyledon opening during de-etiolation in Arabidopsis. Plant Cell **31:** 1155–1170.

Fan, D., Ran, L., Hu, J., Ye, X., Xu, D., Li, J., Su, H., Wang, X., Ren, S., and Luo, K. (2020). The miR319a/TCP module and DELLA protein regulate synergistically trichome initiation and improve insect defenses in *Populus tomentosa*. New Phytol. **227:** 867–883.

Glauser, G., Dubugnon, L., Mousavi, S.A., Rudaz, S., Wolfender, J.L., and Farmer, E.E. (2009). Velocity estimates for signal propagation leading to systemic jasmonic acid accumulation in wounded Arabidopsis. J. Biol. Chem. **284:** 34506–34513.

Guo, Z., Sun, X., and Xu, H. (2018). Gateway-compatible inducible vector set for the functional analysis of transcription factors in plants. Planta **247:** 1261–1266.

Guo, Z., Xu, H., Lei, Q., Du, J., Li, C., Wang, C., Yang, Y., Yang, Y., and Sun, X. (2020). The Arabidopsis transcription factor LBD15 mediates ABA signaling and tolerance of water-deficit stress by regulating *ABI4* expression. Plant J. **104:** 510–521.

Heijde, M., and Ulm, R. (2013). Reversion of the Arabidopsis UV-B photoreceptor UVR8 to the homodimeric ground state. Proc. Natl. Acad. Sci. U. S. A. **110:** 1113–1118.

Hu, Y., Jiang, Y., Han, X., Wang, H., Pan, J., and Yu, D. (2017). Jasmonate regulates leaf senescence and tolerance to cold stress: Crosstalk with other phytohormones. J. Exp. Bot. **68:** 1361–1369.

Huang, X., Ouyang, X., Yang, P., Lau, O.S., Chen, L., Wei, N., and Deng, X.W. (2013). Conversion from CUL4-based COP1-SPA E3 apparatus to UVR8-COP1-SPA complexes underlies a distinct biochemical function of COP1 under UV-B. Proc. Natl. Acad. Sci. U. S. A. **110:** 16669–16674.

Jenkins, G.I. (2014). The UV-B photoreceptor UVR8: From structure to physiology. Plant Cell **26:** 21–37.

Kubota, A., Ito, S., Shim, J.S., Johnson, R.S., Song, Y.H., Breton, G., Goralogia, G.S., Kwon, M.S., Laboy Cintron, D., Koyama, T., et al. (2017). TCP4-dependent induction of CONSTANS transcription requires GIGANTEA in photoperiodic flowering in Arabidopsis. PLoS Genet. **13:** e1006856.

Lan, J., Zhang, J., Yuan, R., Yu, H., An, F., Sun, L., Chen, H., Zhou, Y., Qian, W., He, H., et al. (2021). TCP transcription factors suppress cotyledon trichomes by impeding a cell differentiation-regulating complex. Plant Physiol. **186:** 434–451.

Li, Z., Li, B., Shen, W.H., Huang, H., and Dong, A. (2012). TCP transcription factors interact with AS2 in the repression of class-I KNOX genes in *Arabidopsis thaliana*. Plant J. **71:** 99–107.

Liang, T., Mei, S., Shi, C., Yang, Y., Peng, Y., Ma, L., Wang, F., Li, X., Huang, X., Yin, Y., et al. (2018). UVR8 Interacts with BES1 and BIM1 to regulate transcription and photomorphogenesis in Arabidopsis. Dev. Cell **44:** 512–523 e515.

Liang, T., Shi, C., Peng, Y., Tan, H., Xin, P., Yang, Y., Wang, F., Li, X., Chu, J., Huang, J., et al. (2020). Brassinosteroid-activated BRI1-EMS-SUPPRESSOR 1 inhibits flavonoid biosynthesis and coordinates growth and UV-B stress responses in plants. Plant Cell **32:** 3224–3239.

Liang, T., Yang, Y., and Liu, H. (2019). Signal transduction mediated by the plant UV-B photoreceptor UVR8. New Phytol. **221:** 1247–1252.

Liu, J., Cheng, X., Liu, P., Li, D., Chen, T., Gu, X., and Sun, J. (2017). MicroRNA319-regulated TCPs interact with FBHs and PFT1 to activate CO transcription and control flowering time in Arabidopsis. PLoS Genet. **13:** e1006833.

Liu, X., Chi, H., Yue, M., Zhang, X., Li, W., and Jia, E. (2012). The regulation of exogenous jasmonic acid on UV-B stress tolerance in wheat. J. Plant Growth Regul. **31:** 436–447.

Liu, Y., Li, D., Yan, J., Wang, K., Luo, H., and Zhang, W. (2019). MiR319 mediated salt tolerance by ethylene. Plant. Biotechnol. J. **17:** 2370–2383.

Mackerness, S.-A.H., Surplus, S.L., Blake, P., John, C.F., Buchanan-Wollaston, V., Jordan, B.R., and Thomas, B. (1999). Ultraviolet-B-induced stress and changes in gene expression in *Arabidopsis thaliana*: Role of signalling pathways controlled by jasmonic acid, ethylene and reactive oxygen species. Plant, Cell Environ. **22:** 1413–1423.

Nag, A., King, S., and Jack, T. (2009). miR319a targeting of TCP4 is critical for petal growth and development in Arabidopsis. Proc. Natl. Acad. Sci. U. S. A. **106:** 22534–22539.

Ori, N., Cohen, A.R., Etzioni, A., Brand, A., Yanai, O., Shleizer, S., Menda, N., Amsellem, Z., Efroni, I., Pekker, I., et al. (2007). Regulation of LANCEOLATE by miR319 is required for compound-leaf development in tomato. Nat. Genet. **39:** 787–791.

Palatnik, J.F., Allen, E., Wu, X., Schommer, C., Schwab, R., Carrington, J.C., and Weigel, D. (2003). Control of leaf morphogenesis by microRNAs. Nature **425:** 257–263.

Qi, J., Li, J., Han, X., Li, R., Wu, J., Yu, H., Hu, L., Xiao, Y., Lu, J., and Lou, Y. (2016). Jasmonic acid carboxyl methyltransferase regulates development and herbivory-induced defense response in rice. J. Integr. Plant Biol. **58:** 564–576.

Qi, T., Song, S., Ren, Q., Wu, D., Huang, H., Chen, Y., Fan, M., Peng, W., Ren, C., and Xie, D. (2011). The jasmonate-ZIM-domain proteins interact with the WD-repeat/bHLH/MYB complexes to regulate jasmonate-mediated anthocyanin accumulation and trichome initiation in *Arabidopsis thaliana*. Plant Cell **23:** 1795–1814.

Qian, C., Chen, Z., Liu, Q., Mao, W., Chen, Y., Tian, W., Liu, Y., Han, J., Ouyang, X., and Huang, X. (2020). Coordinated transcriptional regulation by the UV-B photoreceptor and multiple transcription factors for plant UV-B responses. Mol. Plant **13:** 777–792.

Quan, J., Song, S., Abdulrashid, K., Chai, Y., Yue, M., and Liu, X. (2018). Separate and combined response to UV-B radiation and jasmonic acid on photosynthesis and growth characteristics of *Scutellaria baicalensis*. Int. J. Mol. Sci. **19:** 1194.

Ren, H., Han, J., Yang, P., Mao, W., Liu, X., Qiu, L., Qian, C., Liu, Y., Chen, Z., Ouyang, X., et al. (2019). Two E3 ligases antagonistically regulate the UV-B response in *Arabidopsis*. Proc. Natl. Acad. Sci. U. S. A. **116:** 4722–4731.

Rizzini, L., Favory, J.J., Cloix, C., Faggionato, D., O'Hara, A., Kaiserli, E., Baumeister, R., Schafer, E., Nagy, F., Jenkins, G.I., et al. (2011). Perception of UV-B by the Arabidopsis UVR8 protein. Science **332:** 103–106.

Saini, K., Dwivedi, A., and Ranjan, A. (2022). High temperature restricts cell division and leaf size by coordination of PIF4 and TCP4 transcription factors. Plant Physiol. **190:** 2380–2397.

Sarvepalli, K., and Nath, U. (2011). Hyper-activation of the TCP4 transcription factor in *Arabidopsis thaliana* accelerates multiple aspects of plant maturation. Plant J. **67:** 595–607.

Schommer, C., Debernardi, J.M., Bresso, E.G., Rodriguez, R.E., and Palatnik, J.F. (2014). Repression of cell proliferation by miR319-regulated TCP4. Mol. Plant **7:** 1533–1544.

Schommer, C., Palatnik, J.F., Aggarwal, P., Chetelat, A., Cubas, P., Farmer, E.E., Nath, U., and Weigel, D. (2008). Control of jasmonate biosynthesis and senescence by miR319 targets. PLoS Biol. **6:** e230.

Schreiner, M., Mewis, I., Neugart, S., Zrenner, R., Glaab, J., Wiesner, M., and Jansen, M.A.K. (2016). UV-B elicitation of secondary plant metabolites. In *III-Nitride Ultraviolet Emitters: Technology and Applications*, M. Kneissl, J. Rass, eds, (Cham: Springer International Publishing), pp. 387–414.

Seltmann, M.A., Stingl, N.E., Lautenschlaeger, J.K., Krischke, M., Mueller, M.J., and Berger, S. (2010). Differential impact of lipoxygenase 2 and jasmonates on natural and stress-induced senescence in Arabidopsis. Plant Physiol. **152:** 1940–1950.

Shamala, L.F., Zhou, H.C., Han, Z.X., and Wei, S. (2020). UV-B induces distinct transcriptional re-programing in UVR8-signal transduction, flavonoid, and terpenoids pathways in *Camellia sinensis*. Front. Plant Sci. **11:** 234.

Soriano, G., Cloix, C., Heilmann, M., Nunez-Olivera, E., Martinez-Abaigar, J., and Jenkins, G.I. (2018). Evolutionary conservation of structure and function of the UVR8 photoreceptor from the liverwort *Marchantia polymorpha* and the moss *Physcomitrella patens*. New Phytol. **217:** 151–162.

Sun, X., Wang, C., Xiang, N., Li, X., Yang, S., Du, J., Yang, Y., and Yang, Y. (2017). Activation of secondary cell wall biosynthesis by miR319-targeted TCP4 transcription factor. Plant. Biotechnol. J. **15:** 1284–1294.

Teng, S., Keurentjes, J., Bentsink, L., Koornneef, M., and Smeekens, S. (2005). Sucrose-specific induction of anthocyanin biosynthesis in Arabidopsis requires the MYB75/PAP1 gene. Plant Physiol. **139:** 1840–1852.

Thiebaut, F., Rojas, C.A., Almeida, K.L., Grativol, C., Domiciano, G.C., Lamb, C.R., Engler Jde, A., Hemerly, A.S., and Ferreira, P.C. (2012). Regulation of miR319 during cold stress in sugarcane. Plant Cell Environ. **35:** 502–512.

Tissot, N., and Ulm, R. (2020). Cryptochrome-mediated blue-light signalling modulates UVR8 photoreceptor activity and contributes to UV-B tolerance in Arabidopsis. Nat. Commun. **11:** 1323.

Vadde, B.V.L., Challa, K.R., and Nath, U. (2018). The TCP4 transcription factor regulates trichome cell differentiation by directly activating GLABROUS INFLORESCENCE STEMS in *Arabidopsis thaliana*. Plant J. **93:** 259–269.

Yang, C., Li, D., Mao, D., Liu, X., Ji, C., Li, X., Zhao, X., Cheng, Z., Chen, C., and Zhu, L. (2013). Overexpression of microRNA319 impacts leaf morphogenesis and leads to enhanced cold tolerance in rice (*Oryza sativa* L.). Plant Cell Environ. **36:** 2207–2218.

Yang, Y., Zhang, L., Chen, P., Liang, T., Li, X., and Liu, H. (2020). UV-B photoreceptor UVR8 interacts with MYB73/MYB77 to regulate auxin responses and lateral root development. EMBO J. **39:** e101928.

Yang, Y., Liang, T., Zhang, L., Shao, K., Gu, X., Shang, R., Shi, N., Li, X., Zhang, P., and Liu, H. (2018). UVR8 interacts with WRKY36 to regulate HY5 transcription and hypocotyl elongation in Arabidopsis. Nat. Plants **4:** 98–107.

Yin, R., Skvortsova, M.Y., Loubery, S., and Ulm, R. (2016). COP1 is required for UV-B-induced nuclear accumulation of the UVR8 photoreceptor. Proc. Natl. Acad. Sci. U. S. A. **113:** E4415–E4422.

Zhai, Q., Yan, L., Tan, D., Chen, R., Sun, J., Gao, L., Dong, M.Q., Wang, Y., and Li, C. (2013). Phosphorylation-coupled proteolysis of the transcription factor MYC2 is important for jasmonate-signaled plant immunity. PLoS Genet. **9:** e1003422.

Zheng, X., Lan, J., Yu, H., Zhang, J., Zhang, Y., Qin, Y., Su, X.D., and Qin, G. (2022). Arabidopsis transcription factor TCP4 represses chlorophyll biosynthesis to prevent petal greening. Plant Commun. **3:** 100309.

Zhou, M., Li, D., Li, Z., Hu, Q., Yang, C., Zhu, L., and Luo, H. (2013). Constitutive expression of a miR319 gene alters plant development and enhances salt and drought tolerance in transgenic creeping bentgrass. Plant Physiol. **161:** 1375–1391.

Zhou, Y., Xun, Q., Zhang, D., Lv, M., Ou, Y., and Li, J. (2019). TCP transcription factors associate with PHYTOCHROME INTERACTING FACTOR 4 and CRYPTOCHROME 1 to regulate thermomorphogenesis in *Arabidopsis thaliana*. iScience **15:** 600–610.

SUPPORTING INFORMATION

Additional Supporting Information may be found online in the supporting information tab for this article: http://onlinelibrary.wiley.com/doi/10.1111/jipb.13648/suppinfo

Figure S1. Interaction between TCP4 and UV RESISTANCE LOCUS 8 (UVR8) in yeast two-hybrid assays

Figure S2. Anthocyanin accumulation

Figure S3. Identification of homozygous *uvr8* in *rTCP4-3/uvr8* plants

Figure S4. TEOSINTE BRANCHED1, Cycloidea and PCF 4 (TCP4) upregulates jasmonate (JA) content

Figure S5. Anthocyanin contents of 2-week-old seedlings of the wild type (WT), *lox2*, miR319-resistant TEOSINTE BRANCHED1, Cycloidea and PCF 4-3 (rTCP4-3), and rTCP4-3/*lox2*

Figure S6. Quantitative real-time polymerase chain reaction analysis of *LOX2* and WD40/bHLH/R2R3-MYB (WBM) genes *MYB75*, *GL1*, *TT8*, *GL3*, and *EGL3* in wild type (WT), *lox2*, *rTCP4-3*, and miR319-resistant TEOSINTE BRANCHED1, Cycloidea and PCF 4-3 (rTCP4-3)/*lox2*

Table S1. Sequence of primers used in this study